Unraveling reproducible dynamic states of individual brain functional parcellation

Amal Boukhdhir[1,2], Yu Zhang[1,3], Max Mignotte[3], Pierre Bellec[1,3]

1 Centre de recherche de l'institut universitaire de gériatrie de Montréal, Montréal, Québec, Canada.
2 Département d'informatique et de recherche opérationnelle, Université de Montréal, Montréal, Québec, Canada.
3 Département de psychologie, Université de Montréal, Montréal, Québec, Canada.

Abstract

Data-driven parcellations are widely used for exploring the functional organization of the brain, and also for reducing the high dimensionality of fMRI data. Despite the flurry of methods proposed in the literature, functional brain parcellations are not highly reproducible at the level of individual subjects, even with very long acquisitions. Some brain areas are also more difficult to parcellate than others, with association heteromodal cortices being the most challenging. An important limitation of classical parcellations is that they are static, i.e. they neglect dynamic reconfigurations of brain networks. In this paper, we proposed a new method to identify dynamic states of parcellations, which we hypothesized would improve reproducibility over static parcellation approaches. For a series of seed voxels in the brain, we applied a cluster analysis to regroup short (3 minutes) time windows into "states" with highly similar seed parcel. We splitted individual time series of the Midnight Scan Club sample into two independent sets of 2.5 hours (test and retest). We found that average within-state parcels, called stability maps, were highly reproducible (over .9 test-retest spatial correlation in many instances) and subject specific (fingerprinting accuracy over 70% on average) between test and retest. Consistent with our hypothesis, seeds in heteromodal cortices (posterior and anterior cingulate) showed a richer repertoire of states than unimodal (visual) cortex. Taken together, our results indicate that static functional parcellations are incorrectly averaging well defined and distinct dynamic states of brain parcellations. This work calls to revisit previous methods based on static parcellations, which includes the majority of published network analyses of fMRI data. Our method may thus impact how researchers model the rich interactions between brain networks in health and disease.

1. Introduction

Brain parcellation is a tool for understanding the functional organization of the human cerebral cortex, and also to reduce the dimensionality of fMRI data. Parcellations are notably heavily used to characterize brain network properties. A good parcellation should typically satisfy two conflicting objectives. The first objective is to be reproducible enough to allow for replication and comparison across studies. The second objective is to be flexible enough to accurately represent the organization of an individual brain. Simultaneously achieving these

two objectives is challenging, in part due to inter-subject variability [1–3], which is also associated with measures of cognitive performance [4]. In addition, it has also become apparent that brain functional connectivity substantially reorganizes dynamically [5] according to different cognitive states [6]. Our main objective in this work was to develop a new method to capture reproducible dynamic states of parcellations at the individual level. These dynamic states represent the spatial brain reconfigurations over time in the resting state condition.

In the past decade, there has been an explosion of interest in brain parcellation, and parcellation atlases are widely used in computational neuroscience research. This interest dates back to at least a century, with the Broadman atlas [7]. Many popular functional parcellations have been generated at the group level, by averaging the connectivity patterns over many subjects, such as the Yeo-Krienen [8], MIST [9], Glasser [10] and Schaffer atlases [11], amongst many others [12]. Researchers have proposed competing approaches to generate such group parcellations, with improvement measured in terms of reproducibility and homogeneity of the parcels across datasets and subjects, e.g. [13,14]. Even though group parcellations are still widely used, it is now well established that there is a considerable inter-subject variability, which is not properly accounted for through anatomical alignment [15]. Therefore, subject-level parcellation is an active field of research in the brain parcellation community, which aims at accounting for inter-subject variability in brain parcels. It is important to study this brain variability since it was considered as a key feature in predicting behavior, cognition and personality across subjects [4,6,16–18]. Kong and colleagues, for instance, estimated subject-specific parcels using a multi-session hierarchical bayesian model [17]. Also, Dickie et al. suggested an approach for identifying subject specific resting-state networks in fMRI, and their results showed a higher variability in the spatial locations of resting-state networks within individuals with autism spectrum disorder patients compared with control individuals [19]. The literature on this topic is too vast to be systematically reviewed here, but we refer interested readers to Eickhoff and colleagues [20] for a more extensive review.

Even though there has been remarkable progress in the field of brain parcellation, there are still concerns about the reproducibility of individual level parcellations. For instance, Gordon and colleagues confirmed that subject-to-group similarity was relatively low [21]. This was measured by the average parcel connectivity similarity to group connectivity score, which reached a plateau with an average of 0.7 for long scan duration (~ 800 timepoints) [15]. Researchers reported that the lateral prefrontal cortex and the lateral temporal occipital cortex were among the most variable parcels across subjects [22]. We hypothesize that the main limitation of these approaches was the use of a fixed parcellation over time, which neglected the dynamic aspect of heteromodal brain networks [6]. In other words, different brain reconfigurations for each parcel were forced to be averaged in one brain parcel while suppressing region boundaries reconfigurations over time. In the literature, Yeo and colleagues reported results in line with our hypothesis, showing that brain networks were continually aggregating and segregating over time [23]. This suggests the importance of considering the dynamic aspects of brain parcellation, rather than considering it as a fixed system.

A proliferation of approaches also exist in the literature to study the dynamics of functional connectivity. These studies confirmed the spatio temporal reconfiguration of the brain networks [24–27] and associated it to dynamics of cognitive processing or mental states dictated by tasks [28–32]. The co-activation patterns [33,34], spatial independent component analysis [35] were among the most widely applied techniques to consider brain dynamics (see [36] for a review). These dynamic analyses of the brain, using for instance sliding window correlation, have demonstrated better results compared to stationary approaches in the detection of neurological disease [37,38]. Other findings confirmed the interaction between brain networks for different task states [1,23,39]. For instance, Braga and Buckner discovered that the default mode network could be reliably subdivided into parallel networks within the same individual [1]. Chen and colleagues modeled these states switching processes of resting state brain activities using a hidden markov model [33]. Therefore, neuroscientists mentioned there is a need to have neuroimaging tools to identify how brain parcels reconfigure spatially in the case of highly cognitive regions over time and to evaluate the variability of brain parcels across time and across individuals [32]. Even though dynamic functional connectivity is well studied, to the best of our knowledge, the only parcellation approach that considered dynamic changes of parcels was suggested by Salehi and colleagues. These authors demonstrated that the brain functional parcellations are not spatially fixed, but reconfigure with task conditions [6,40]. These reconfigurations were used to reliably predict different task conditions. Still, this approach only suggested a brain parcellation per task condition, and it neglected brain parcel reconfigurations across short time durations, within each task. Dynamic brain parcellation thus represents a promising area of research to further investigate brain dynamics.

In this paper, we build upon the findings of Salehi and colleagues [6], and we propose a novel approach to extract different dynamic states of functional parcellations at the individual level. We define a dynamic state of parcellation as the spatial reconfiguration of a given brain network that occurs for short time durations in the resting state condition. We hypothesize the existence of homogeneous modes of spatial reconfigurations, or dynamic states of parcellations, at the level of these short time windows and we propose a dynamic cluster analysis for their identification. Our approach is based on aggregating sliding-window parcellations for a given region to obtain stability maps of the different dynamic states of parcellations. We generate these dynamic states for the ten subjects of the Midnight Scan Club (MSC) resting-state dataset and we aim to study similarities and variations within-state (across replication sets), across states (within-subject), and across subjects. We also aim to evaluate the reliability of the generated states maps in a “fingerprinting” experiment, i.e. matching state maps generated from the same subjects within a group.

2. Materials and methods

2.1 Dataset and preprocessing

The resting-state MSC dataset includes ten healthy subjects (female=5, male=5, their age ranges between 24-34 years old [15]. Informed consent was obtained from all participants. The study was approved by the Washington University School of Medicine Human Studies

Committee and Institutional Review Board [15]. Each subject underwent a total of five hours of resting state functional MRI data, with a series of 30 minutes contiguous acquisitions, beginning at midnight for ten consecutive days. In each session, subjects visually fixated on a white crosshair presented against a black background. All functional imaging was performed using a gradient-echo EPI sequence (TR = 2.2s, TE = 27 ms, flip angle = 90°, voxel size = 4 mm × 4 mm × 4 mm, 36 slices) on a Siemens TRIO 3T MRI scanner. An EyeLink 1000 eye-tracking system allowed continuous monitoring of the eyes of the subjects in order to check for periods of prolonged eye closure, potentially indicating sleep. Only one subject (MSC08) demonstrated prolonged eye closures. For details about the data acquisition parameters see [15]. The MSC dataset was preprocessed and analyzed using the NeuroImaging Analysis Kit[1] executed within a Ubuntu 16.0.4 Singularity container, running GNU Octave version 4.2.1, and the MINC toolkit version 1.9.15. The first five volumes of each run were suppressed to allow the magnetisation and reach equilibrium. Time series were normalized to the zero mean and unit variance. Each fMRI session was corrected of inter-slice difference in acquisition time and the parameters of a rigid-body motion was estimated for each time frame. The "scrubbing" method of [41], was used to remove the volumes with excessive motion (frame displacement greater than 0.5). No session was excluded due to excessive motion. Each session had at least 420 volumes after scrubbing, across all subjects, and with a maximum of 810 volumes available. Also, the nuisance parameters were regressed out from the time series at each voxel i.e., slow time drifts, average signals in conservative masks of the white matter and the lateral ventricles, as well as the first principal components of the six rigid-body motion parameters and their squares. The fMRI volumes were spatially smoothed with a 6 mm isotropic Gaussian blurring kernel.A more detailed description of the preprocessing pipeline can be found on the NIAK website[2].

2.2 Individual dynamic states of parcellation

We developed an algorithm which identifies dynamic states of brain parcellation at the individual level. The algorithm is composed of four steps as illustrated in Fig. 1. In the first step (Fig. 1A), we select a series of sliding time windows from individual fMRI time series ($W=100$ time points, with $O=10$ time points of overlap, starting from the first time point), and we generate parcels for the whole cerebral cortex using a k-means clustering algorithm[42]. We select fMRI time windows from several runs, such that some time series may combine signals from separate runs. The motivation behind this parcellation step is the identification of brain regions with similar temporal activity for a given time window. We choose the k-means for its linear complexity and simplicity to run; i.e. no need for many parameters to tune [43,44]. Our algorithm is parallelized based on the multiprocessing library to run computations on multiple cores[3]. We also used kmeans using scikit-learn implementation[4] [42] to generate parcellations and used the k-means++ method to choose initial cluster centers in a strategic way, in order to speed-up convergence. Although the k-means algorithm has the drawback of falling into local minima, the k-means++ initialization helps

[1] https://hub.docker.com/r/simexp/niak-cog/
[2] http://niak.simexp-lab.org/pipe_preprocessing.html
[3] https://docs.python.org/3.4/library/multiprocessing.html?highlight=process
[4] https://scikit-learn.org/stable/modules/generated/sklearn.cluster.KMeans.html

overcome this limitation with a better exploration of the parcellation solution search space. We also replicate the parcellation (repetition = 5) for each window with different initializations of the random number generator, which will help identify consistent solutions across different local minima.

In the second step (Fig. 1B), we identify, for a particular seed voxel, which parcel this voxel is associated with. We thus obtain a binary representation called seed-based parcellation. This step may contribute to the success of our approach, since it allows us to simplify the complexity of the full brain parcellation problem by focusing on the functional activity of one region of interest.

In the third step (Fig. 1C), we calculate the pairwise similarity of all seed-based parcellations generated from different sliding windows. This similarity is measured with the so-called Dice similarity score. Then, we apply the Hierarchical clustering (here, with the average linkage method) on the Dice-similarity matrix to group seed-based parcellations into dynamic clusters, according to an empirical similarity threshold. This threshold constrains the clustering by requiring a minimum Dice similarity (here, 0.3) between seed-based parcels in the same dynamic cluster, which will in turn infer the number of dynamic clusters in a data-driven way. Given the previously mentioned settings, we hypothesized that some clusters would have few sliding windows i.e., inferior to 10% of the total number of available sliding windows. Therefore, these clusters are more likely to represent spurious or noisy spatial configurations, or simply not too infrequent to be to be estimated properly. We then apply another threshold to keep only dynamic states with more than 10% of sliding windows. This second threshold will remove noisy states in order to keep only reproducible patterns over time. There should be a trade-off between the similarity threshold imposed on the Dice similarity matrix and the threshold that constrained the final number of dynamic states or the cluster size. In other words, a higher Dice score threshold allows to obtain smaller size clusters (or dynamic states of parcellations) and thus, requires smaller cluster size threshold to avoid missing the most interesting clusters.

In the last step (Fig. 1D), we averaged all seed-based parcels for a given cluster to get its state stability map. This provides a probability of each voxel to be assigned to a given state as a measure of the stability of voxels with respect to their membership in a particular area. Stability maps represent the spatial signature of each dynamic state of brain parcellations, and the final outcome of the algorithm.

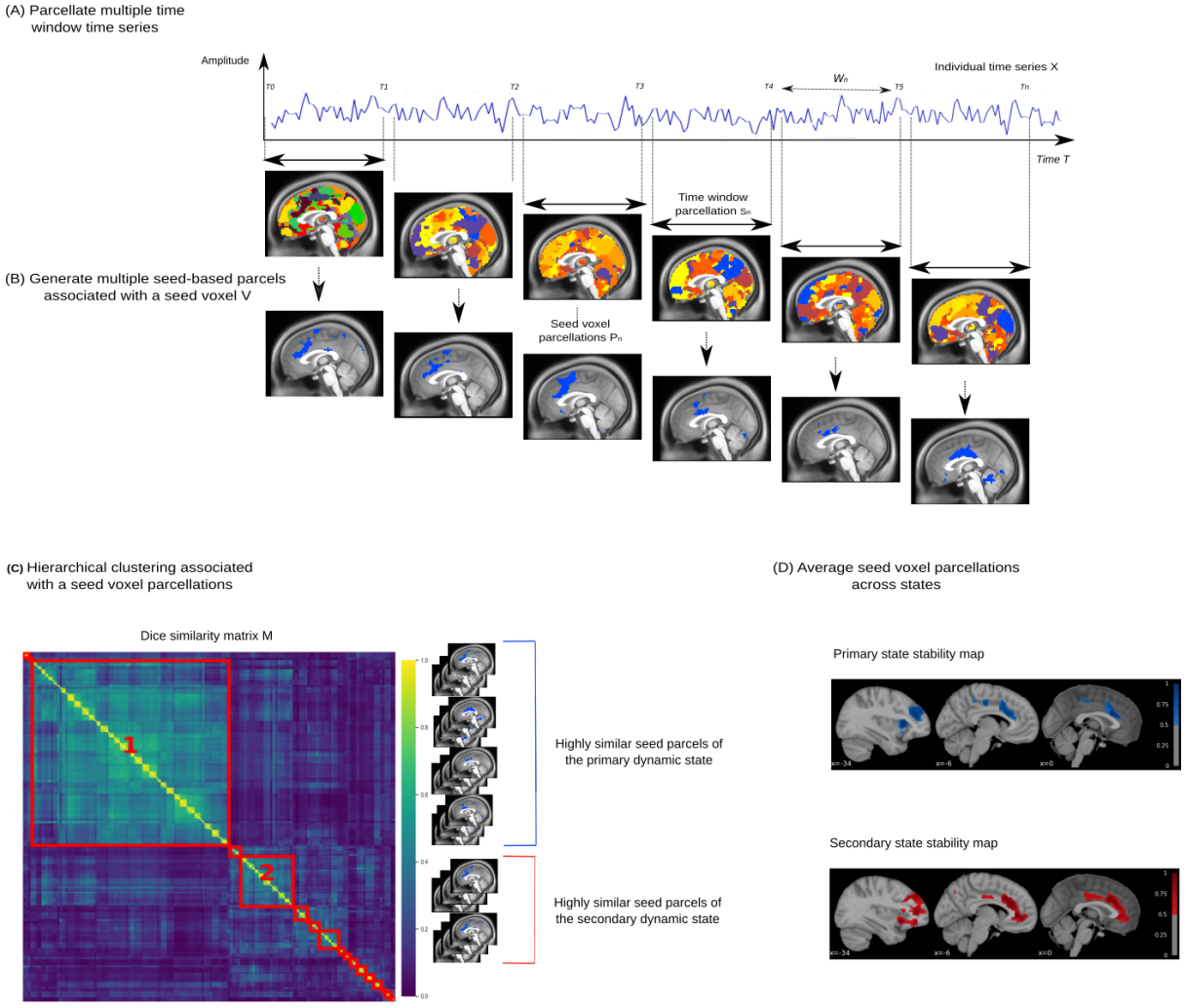

Figure 1. Subject-specific dynamic parcellation approach; (A) we generate multiple short time window parcels for the whole cerebral cortex per subject. (B) Then, we identify the parcel associated with a particular seed-voxel. (C) We calculate the pairwise similarity of these seed-based parcellations based on the Dice similarity score. (D) we apply a Hierarchical clustering on this similarity matrix to group these parcellations into a set of clusters (or dynamic states of parcellations) according to a threshold imposed on the Dice similarity matrix, as well as the number of sliding windows included in the state. (D) For each cluster and each seed, we average of all its seed-based parcellations to obtain the final dynamic state stability maps.

2.3 Choice of the studied networks and their seed

To generate seed-based parcellations, we studied seed voxels from three regions of the MIST parcellation. We picked MNI coordinates (0, -76, 10), (0, 20, 28) and (3, -43, 37) as the respective medoids of the ROIs 90, 6 and 42 corresponding to the posterior medial visual network (PM-VIS), the dorsal anterior cingulate cortex (dACC) and the posterior cingulate cortex (PCC) networks in the MIST atlas [9]. The choice of seeds is driven by the properties of the networks in the literature. We first chose a seed from an area with the least functional variability [45]: PM-VIS, a core visual area [21]. In the case of the dACC, this region plays a

prominent role within the salience network, which is involved in many functions including response selection, conflict resolution and cognitive control and it is among the most highly dissimilar networks across subjects [45–47]. Finally, the PCC is considered as a hub node in the default mode network. Previous findings reported it as a highly heterogeneous network and suggested it may play a direct role in regulating the focus of attention, memory retrieval, conscious awareness and future planning. Also, functional interaction between the nodes of the salience seed and those of the default mode, including the PCC, during moral reasoning is reported in previous studies [48,49].

2.4 Within and between-subject spatial consistency analysis

To evaluate the quality of the generated dynamic states of parcellations, we conducted a quantitative consistency analysis at the within-subject level. This allowed us to identify, for a given subject, similarities and variations in the spatial reconfigurations across states and seeds. To this end, we half-split our dataset into two equally sized sets of five independent sessions (of a total of 2.5 hours each) per subject. Each half was used to replicate several seed-based parcellations that we called replication set. Then, we generated dynamic states of parcellations based on our proposed approach (See Fig. 1). We sorted the states by decreasing dwell time for the first replication set (i.e. the cumulative durations of all time-windows associated with a given state, relative to the total duration of the scan). Accordingly, we labeled the states of the first replication set into primary, secondary state, tertiary state, etc. Prior to comparing state stability maps, we matched the first set maps to maps from the second set using the Hungarian method [50] which used the Pearson correlation for a spatial matching between state stability maps. A high correlation reflected a strong linear relationship between states maps and is indicative of consistent spatial regions from the two sets of independent data. We replicated these consistency analyses across all states and all subjects of the MSC dataset.

2.5 Fingerprinting experiment

We finally evaluated the individual specificity of our dynamic states of parcellations by attempting to match dynamic states maps generated from data acquired on the same subjects, when these maps are mixed with maps generated from other subjects. To this end, we cross-correlated a given state stability map with all state stability maps from all subjects. A fingerprinting was successful when maximal correlation was observed between the pair of two state stability maps originating from the same subject, otherwise it was considered as a failure. We repeated this experiment for all state maps across all subjects and seeds. We computed the accuracy score as the number of correct states matching over the total number matched maps. A high accuracy score revealed that state stability maps were reliable to differentiate subjects based on their specific spatial brain reconfigurations. Inversely, a low accuracy score was associated with state stability maps which were either very similar across subjects or unreliable within subjects.

2.6 Data records

Scripts used in this study are available on Github[5]. The generation of state stability maps can be executed online via a Jupyter notebook via the binder platform. We have also made available online all the state stability maps for the ten subjects of the MSC dataset on the neurovault website[6].

3. Results

3.1 Temporal cluster analysis reveals "dynamic parcellation states" with highly homogeneous parcels within a state, and highly dissimilar parcels across states

We first aimed to assess whether homogeneous parcels can be extracted from short time windows of about 3 minutes duration. We replicated a seed-based brain parcellation on 220 sliding-windows for this purpose. These time windows were extracted from a pool of time samples, generated by randomly concatenating five sessions of imaging data for the MSC sample, resulting in a total of 2.5 hours of fMRI signals per subject. For a given seed voxel in the brain, we observed pairs of parcels with high homogeneity across different time windows: Dice coefficients between pairs of parcels were larger than 0.8, or 0.9 for some seeds and subjects, see Fig. 2. By contrast, many pairs of parcel replications across time windows had very low Dice score, close to zero, despite being associated with the same seed. For example, in the similarity matrix of subject MSC02, bright colors were associated with some highly homogeneous parcels across the diagonal, while, the remaining pairs of parcels were associated with low Dice values (blue color). This observation motivated us to develop a "dynamic cluster analysis", grouping brain parcels on sliding windows into a number of homogeneous 'dynamic states of parcellations', for a given seed voxel. This approach allowed us to disentangle different dynamic states of brain parcels based on the variability of their spatial distribution over time, specifically for a given brain location. Each dynamic state was also characterized by its dwell time relative to the total scan duration, i.e. the proportion of the total number of sliding windows that were associated with a given state. We applied two criteria to decide on the number of states for a seed voxel: 1) parcels within a state had to exhibit a minimal average level of Dice similarity (i.e. Dice > 0.3), and 2) the dwell time of a given dynamic state needed to be substantial, i.e. larger than 10%. For example, using these two criteria for the PCC seed and subject MSC02, three separate dynamic states of parcellations were identified, and together these dynamic states of parcellations added to about 75% dwell time of all available sliding-windows, see Fig. 2. Taken together, these results showed that resting-state brain parcellations fall into a number of highly homogeneous and distinct states over time, at an individual level.

[5] https://github.com/SIMEXP/dynamic-states-parcellations
[6] https://identifiers.org/neurovault.collection:6642

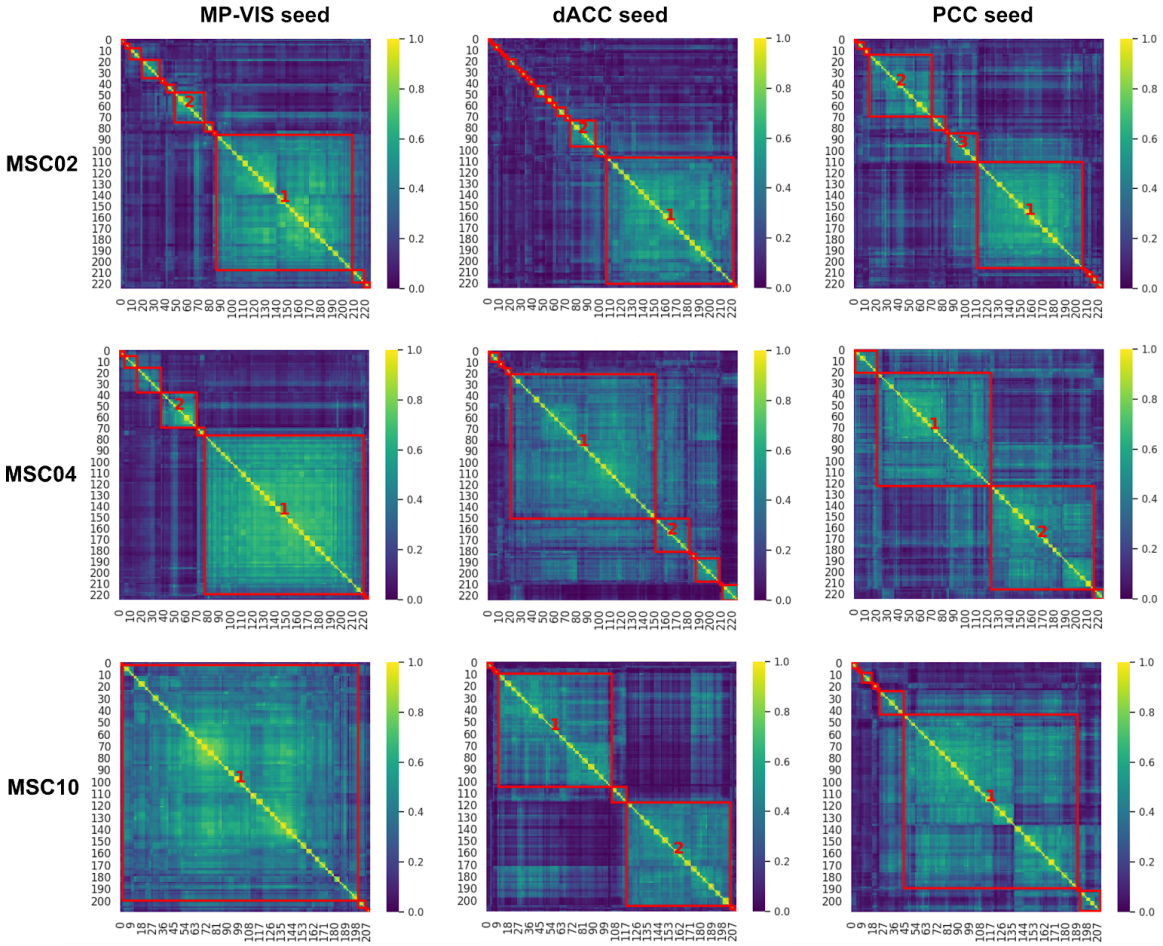

Figure 2. Dice similarity matrices of seed-based brain parcellations showed groups of highly homogeneous parcels and other groups of dissimilar parcels. Each element in the similarity matrix represented the Dice score between a pair of seed-based parcellations. This matrix was calculated separately for each subject and each seed voxel. Three subjects of the MSC dataset and three seeds were investigated i.e.; the Posterior Medial Visual network (PM-VIS), the dorsal Anterior Cingulate (dACC) and the Posterior Cingulate Cortex (PCC).

3.2 Visual evaluation of dynamic states of parcellations within and between subjects

To assess the reproducibility of parcels, the dynamic parcellation method was applied on independent datasets for each subject, each dataset was composed of five sessions (~for a total duration of 2.5 hours of data per subject) available in the MSC sample. We looked at the spatial reconfigurations of dynamic states of parcellations and tried to identify similarities and variations within-state (across replication sets, within subject), across states (within-subject), and across subjects. At the within-state level, we observed a high consistency between the dynamic states of the two replication sets, for all seeds and subjects. For instance, in subject MSC04 and the MP-VIS seed, the primary state maps showed high consistency in the left anterior insula (AI) region (Fig. 3, X=-38) and the supragenual anterior cingulate cortex (sACC) region (Fig. 3, X=-4). Similarly, the secondary

state map of subject MSC02 and the dACC seed had consistent dACC region (Fig. 4, X=-4) and left AI region (Fig. 4, X=-38). Finally, the primary and the tertiary state maps of subject MSC02 and the PCC seed, had respectively consistent TPJ (Fig. 5, X=-38) and MPFC (Fig. 5, X=2) across the two replication sets.

Across states, there existed different spatial reconfigurations within the same subject, especially in the cases of the dACC and PCC seeds. We observed some differences locally, at the level of a region surrounding the seed. For example, the region around the dACC seed was circumscribed and anterior in the primary state of subject MSC02, while the region shifted to the posterior direction in the secondary state (Fig. 4, X=-4). We also observed differences involving multiple regions distributed throughout the brain. Using again the example of subject MSC02 and the dACC seed, the entire AI was involved in the primary state, while the secondary state included only the dorsal anterior insula region (dAI) and the ventral anterior insula (vAI) regions (Fig. 4, X=-38). Similar local and distributed variations were observed with the PCC seed, which had up to three states in the case of subject MSC02 (Fig. 5). The primary state had a cortical region following the boundaries of PCC (Fig. 5, X=-4), along with distributed regions in the cerebellum (Fig. 5, X=38) and the left-temporoparietal junction (TPJ) (Fig. 5, X=-38). By contrast, the tertiary state included the PCC core (Fig. 5, X=-4) along the MPFC (X=2). Finally, the secondary state involved almost exclusively an extensive PCC region (Fig.5, X=-4).

At the inter-subject level, we found some overlapping in regions as well as completely inconsistent regions between subjects in their state spatial maps. As an example of overlapping regions, we found that the MP-VIS seed was characterized by highly similar visual cortex regions for all subjects (Fig. 3). Only subject MSC04 had an inconsistent primary state map that differed from other subjects maps. Here, we observed that the MP-VIS seed involved AI regions (Fig. 3, X=-38) and sACC regions (Fig. 3, X=-4). Unlike the MP-VIS seed, the dACC and the PCC seeds had both overlapping and non-overlapping regions when we compared their state maps across subjects. As an example, we found some overlapping regions in the primary states of subjects MSC02 and MSC10 and the dACC seed (Fig. 4), e.g. overlapping AI region (Fig. 4, X=-38) and dACC region (Fig. 4, X=-4). For the same dACC seed, some subjects had non-overlapping regions such as the secondary states of subject MSC02 and subject MSC10 (Fig. 4). In the secondary state of subject MSC02, the dACC region (Fig. 4, X=-4) occurred as a dominant region along with AI regions (Fig. 4, X=-38). However, the secondary state of subject MSC10 was particularly characterized by the existence of the visual region (Fig 4, X=-9), the anterior hippocampus (AH) and the sACC (Fig. 4, X=-4).

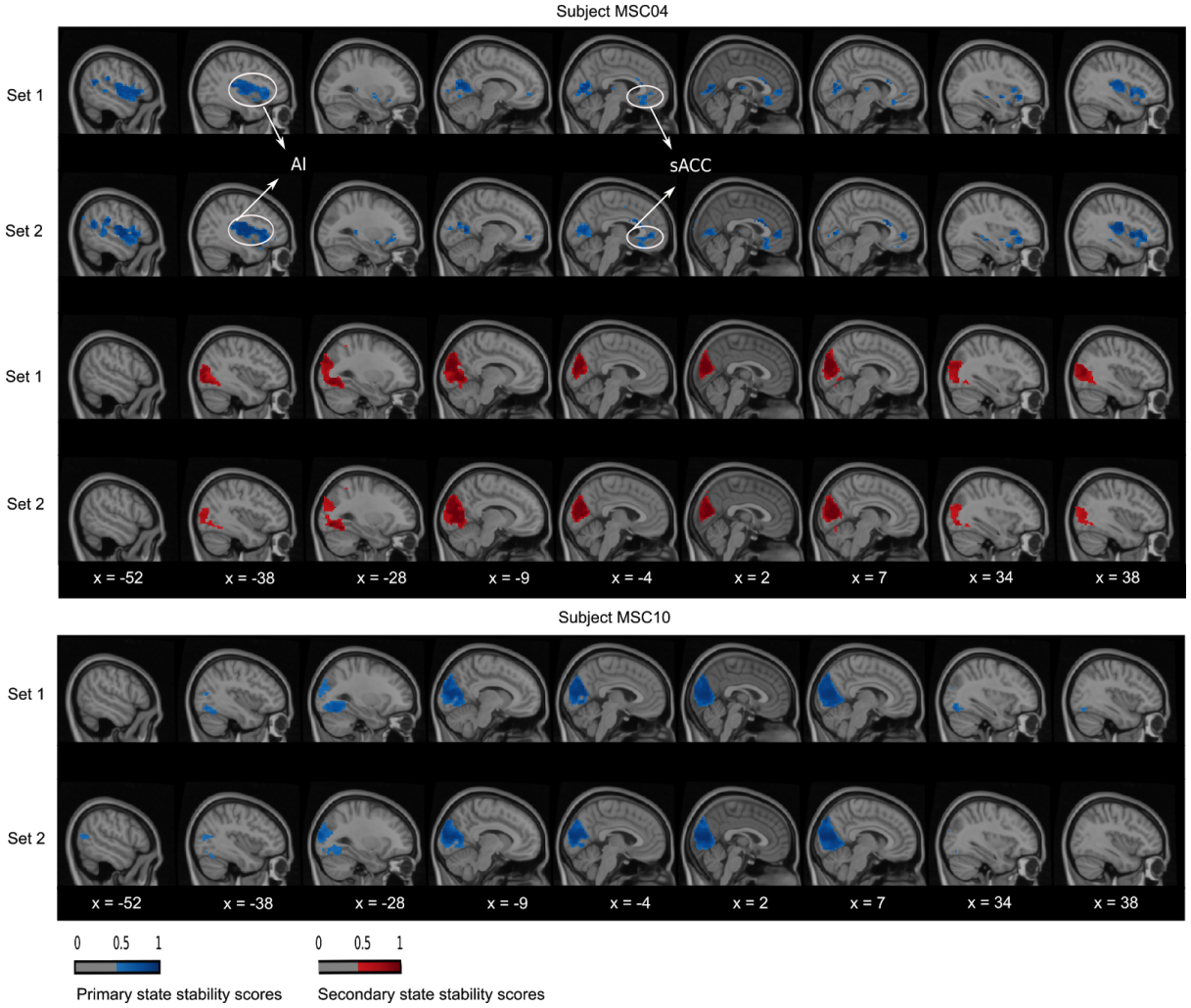

Figure 3. PM-VIS dynamic state stability maps were similar across sets at the within-subject level and variable across states and subjects. A complete matching between states was applied using the Hungarian method by maximizing the Pearson correlation between maps. The primary and secondary states were represented in, respectively, blue and red colors. A threshold was applied to keep only stability scores over 0.5.

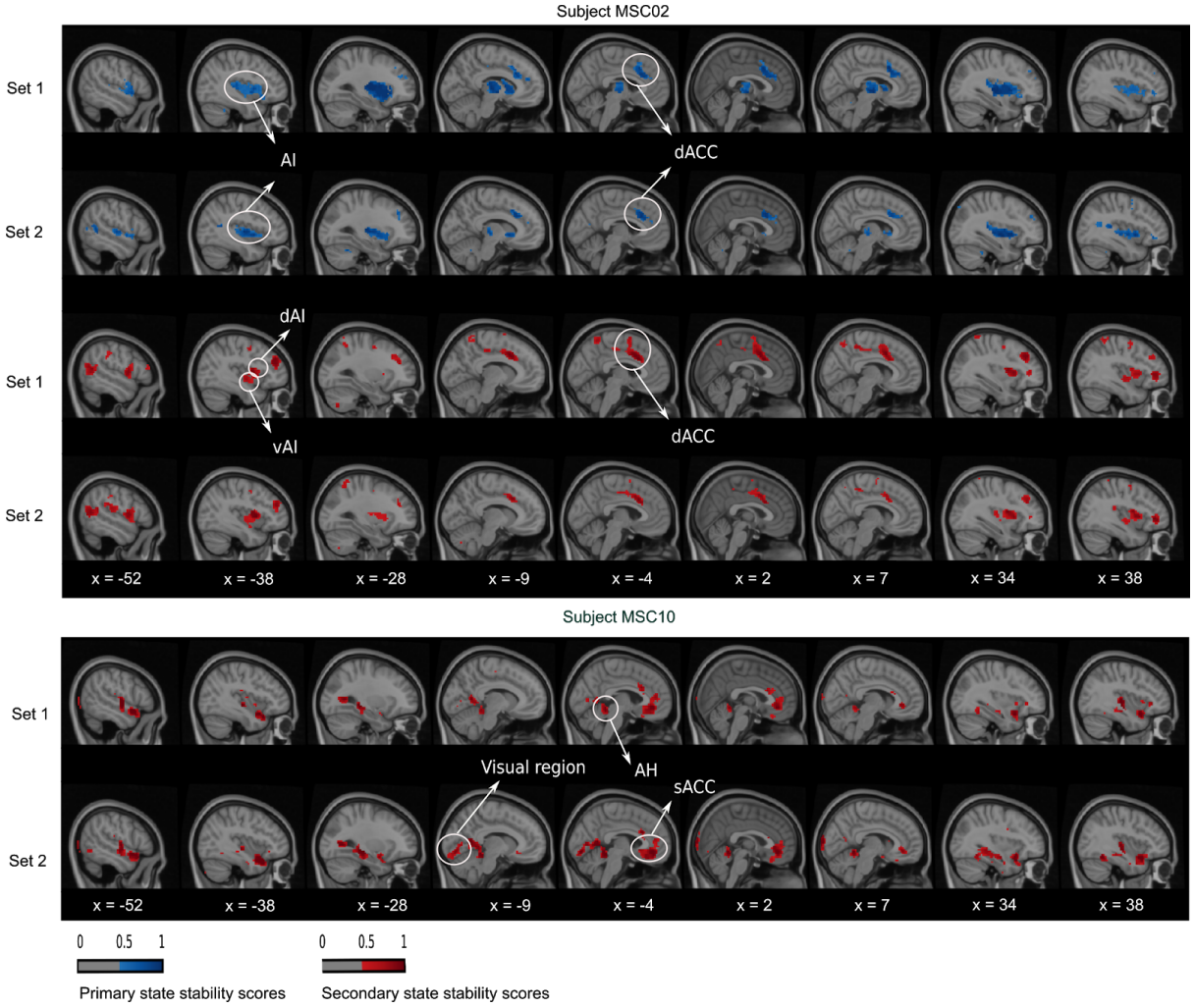

Figure 4. dACC dynamic state stability maps were similar across sets at the within-subject level and variable across states and subjects. A complete matching between states was applied using the Hungarian method by maximizing the Pearson correlation between pairwise maps. The primary and secondary states were represented in, respectively, blue and red colors. A threshold was applied to keep only stability scores over 0.5.

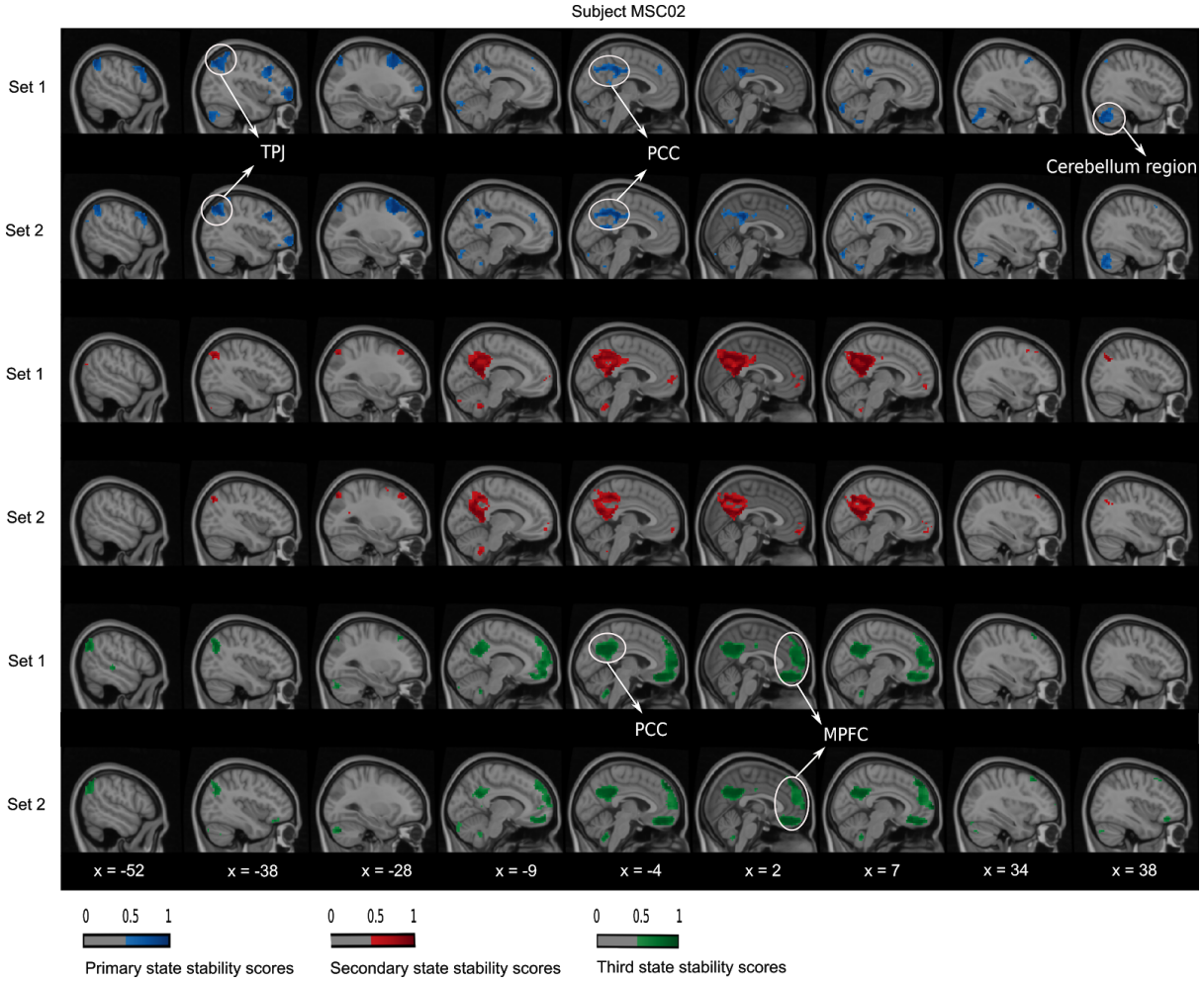

Figure 5. PCC dynamic state stability maps were similar across sets at the within-subject level and variable across states and subjects. The primary, secondary and third states were represented in, respectively, blue, red and green colors. A threshold was applied to keep only stability scores over 0.5.

3.3 Dynamic states of parcellations are highly reproducible at the intra-subject level

We quantified the reproducibility of our dynamic states of parcellations at the within-subject level. First, we computed the within-subject consistency by means of a spatial similarity measure (i.e. Pearson correlation) between state stability maps associated with two sets of five sessions per subject. Each value in the stability map represented the probability of a voxel to belong to the cluster of a given seed. In these maps, we observed a high within-subject reproducibility scores across states and seeds. For instance, most subjects had a reproducibility score that exceeded 0.8 in terms of the Pearson correlation across seeds in the cases of primary and secondary states. Although the third state rarely occurred, it had a high reproducibility score with more than 0.75 reproducibility score, e.g. for the dACC seed, both subjects MSC3 and MSC8 had, respectively, 0.78 and 0.75 Pearson correlation scores. Similarly, for the PCC seed, subject MSC2 had a 0.9 correlation score. The PM-VIS seed was characterized by the highest reproducibility scores compared to the dACC and the PCC with more than 0.9. Except subject MSC04, all subjects had only one

highly reproducible state (see Fig. 6). Some states from one set did not have a matched map from the second set and had, therefore a zero correlation score. For example, in the case of the PM-VIS seed and the primary state, subject MSC02 did not have a state in the replication sample that matched the primary state of the discovery sample (see Fig. 6).

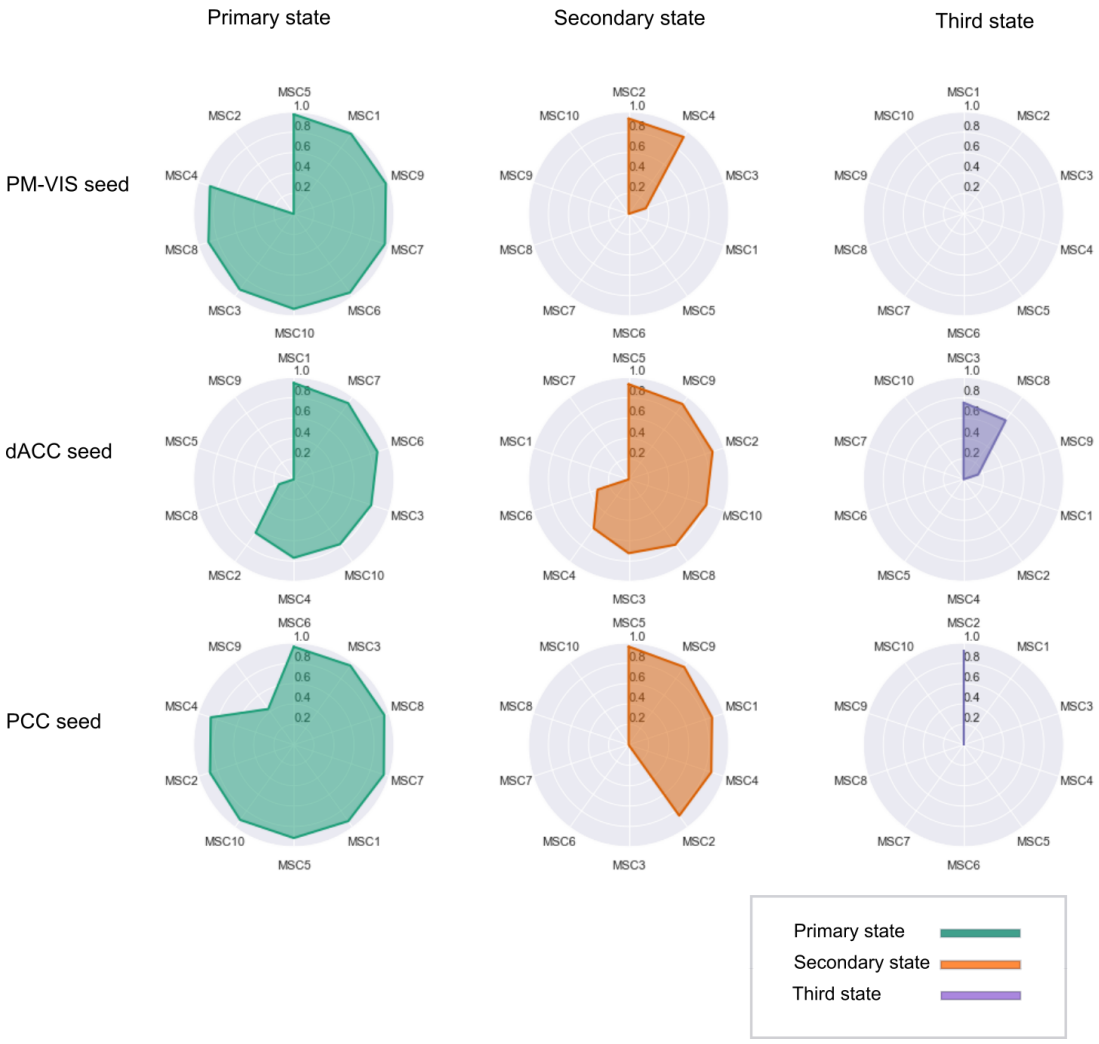

Figure 6. High spatial reproducibility of dynamic states of parcellations across subjects and seeds. Most subjects had two dynamic states of parcellations and the highest reproducibility score was found for the primary states of the three networks including the PM-VIS, the dACC and the PCC seeds. These reproducibility scores represented the similarity between state stability maps associated with two sets of data for each subject. Each set of data included five independent sessions. A complete matching between states was applied using the Hungarian method by maximizing the Pearson correlation between pairwise maps. States were sorted and labeled (i.e., primary state, secondary state, third state, etc.) based on their dwell time such that the primary state had the highest dwell time. Ten subjects of the MSC dataset were investigated i.e.; MSC1, MSC2, MSC3, etc.).

3.4 Within-subject reproducibility of dynamic states of parcellations is substantially higher than between-subject reproducibility

In this section, our purpose was to contrast the dynamic states reproducibility within and between subjects. To this end, we cross-correlated their state stability maps as a measure of reproducibility and compared the results at the inter and within-subject levels. Our results showed that within-subject reproducibility scores outperformed the inter-subject reproducibility scores with almost, two disjoint distributions of correlation scores for all dynamic states and seeds, see Fig. 7. For example, the between-subject PCC-related scores did not exceed 0.65 in the case of the primary state while most within-subject reproducibility scores exceeded 0.8. Similar findings were observed in the case of the dACC. Only a few cases of the within-subject reproducibility scores fell within the distribution of inter-subject reproducibility.

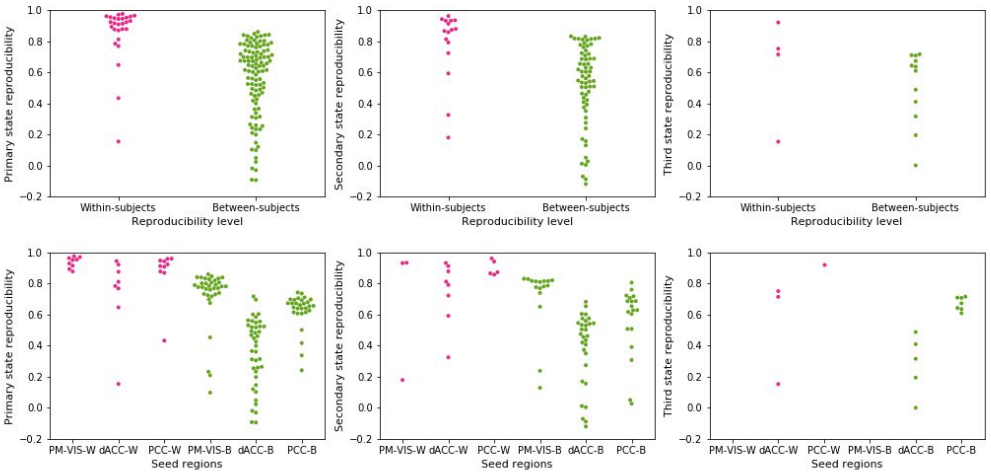

Figure 7. Within-subject reproducibility scores were higher than between-subject reproducibility scores for most dynamic states of parcellations while being overlapped for some states across seeds and subjects. The first row showed the within-subject and between-subject reproducibility scores across three states for three seeds respectively, in pink and green colors (i.e.; PM-VIS, the dACC and the PCC). The second row showed reproducibility scores for each seed, separately such that -W and -B suffixes denoted Within- and Between-subjects reproducibility. A pink dot represented the correlation score of two state stability maps from the same subject while a green one referred to the correlation score of two state maps associated with two different subjects.

3.5 Dynamic state stability maps can reliably identify subjects

We evaluated the reliability of our dynamic state stability maps in identifying a particular subject among a pool of subjects using these maps. The results of this fingerprinting experiment showed high accuracy results for all seeds, with more than 0.7 average accuracy scores. This confirmed that almost all subjects were successfully fingerprinted based on one

of their state maps. The highest accuracy results were associated with the PCC seed with an average of 0.89 across states. The dACC state maps had also a high average accuracy score of 0.75 which meant states maps were helpful in the identification of a particular subject among others. The lowest score was associated with the PM-VIS with an average accuracy of 0.73. In the case of a failure, two state stability maps were highly correlated but their maps were not associated with the same subject. Most failures were associated with the PM-VIS and the dACC. Only a few cases were related to the PCC seed. Overall, these findings confirmed that our dynamic state stability maps were reliable in the delineation of subjects.

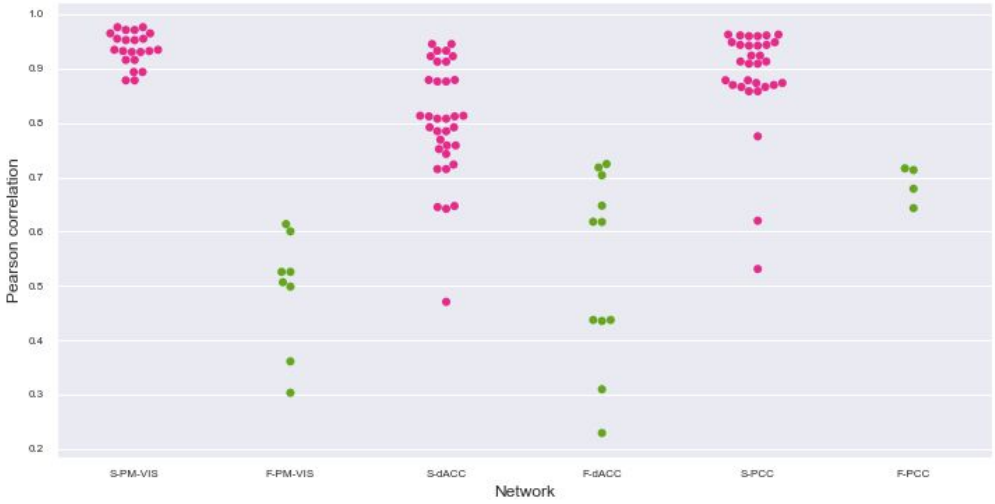

Figure 8. The fingerprinting experiment showed high reliability of state stability maps in delineating subjects across seeds. The spatial similarity was computed between pairs of states stability maps in terms of Pearson correlation. If the correlated maps were associated with the same subject, it was considered a success fingerprinting (pink dots). Otherwise, the correlated maps were associated with different subjects. This was considered a failure (green dots). S- prefix represented a successful fingerprinting in the case of a given network. Conversely, F- prefix represented a failure.

4. Discussion

In this paper, our overall objective was the identification of dynamic states of brain parcellations in individual resting state fMRI data. Our first main finding was the existence of highly similar spatial parcels extracted from short time windows, sometimes separated by several days. This led us to propose a dynamic cluster analysis to extract dynamic states of parcellations. These dynamic states were markedly different in terms of the brain regions involved, despite being derived from the same seed region and the same subject. We also found that dynamic states of parcellations were subject-specific, highly reproducible, and are reliable enough to successfully differentiate subjects in a fingerprinting experiment with high accuracy.

In the literature of brain parcellation, the only approach that had consistent findings with our approach was published by Salehi and colleagues [6,40]. We both suggested an approach that contradicts the notion of a fixed functional parcellation of the brain. The main difference with our work is that Salehi and colleagues generated a different parcellation for different cognitive states in a series of task datasets (i.e. motor task, working memory, rest, etc.), while in our approach we identified different dynamic states of parcellations in short windows of a single cognitive state (resting state). Our results on dynamic brain parcellation is in line with several studies which showed that brain connectivity is highly dynamic, with recurring spatiotemporal patterns of brain networks [24–27]. For instance, Iraji and colleagues demonstrated the existence of spatial fluid interactions between intra- and inter-network relationships, emphasizing the dynamic interplay between segregation and integration [38]. Researchers raised the need for new computational methods to reveal robust, interpretable reconfigurations in the complex and high-dimensional feature space of dynamic fMRI data [36]. Such methods would allow a better understanding of the individual differences in internal state changes over short time scales [36]. In the brain parcellation literature, our approach is, to our knowledge, the first attempt to shed light on this dynamic brain organization at fine temporal scale (in the order of few minutes) and at a voxel level (i.e. without reducing the dimensionality in a fine-grain parcellation).

To evaluate the quality of our dynamic states of parcellations, we relied mainly on a reproducibility analysis. We found that our reproducibility scores markedly outperformed static brain parcellation scores [17]. For instance, the reproducibility scores observed in the case of our visual dynamic states of parcellations were near perfect (with an average correlation scores of 0.95), while visual static brain parcels reported previously in the literature were not (with an average Dice score of 0.85) [17]. Such high reproducibility scores were also observed for all three seeds (See Fig. 7). Another important consideration was that parcels reproducibility depended on the spatial location in the brain in the case of static parcellations, while we observed the same ranges of values for the three seeds. For instance, static parcellations reproducibility ranged between 0.7 and 0.85 average Dice scores in the cases of temporal and visual cortices regions, respectively [17]. Interestingly, our spatial correlation similarity measure exceeded 0.8 for the three seeds for the primary states, and exceeded 0.7 correlation score for secondary and third states for almost all subjects and seeds (See Fig. 7). Recent attempts towards better reproducibility scores of static connectivity measures relied on long fMRI acquisitions [15]. Even though similarity measures were improved (with 10 minutes and 50 minutes of data, authors got, respectively 0.6 and 0.7 average Dice scores), these measures plateaued after ~40 minutes of acquired signal with a maximum average of 0.7 Dice score across the ten subjects of MSC dataset. In our case, higher Dice scores were observed for pairs of seed-based parcels as extracted from a few minutes (~3 minutes) of fMRI data within a given dynamic state. Overall, many studies have aimed to derive static brain parcellation approaches either at the group or the individual level (See [12] and [20] for a review) and yet, no technique had highly reproducible individual parcels. This leads to the conclusion that human brain parcellation is a hard ill-posed problem [12]. Our results demonstrated that the main limitation associated with static brain parcellation approaches is neither the quality of employed clustering algorithms, the quality of fMRI data in specific brain regions nor the duration of fMRI acquisitions. The main issue was the incorrect formalization of functional brain parcellation

as a static problem, which did not take into consideration the dynamic organization of the brain. Specifically, we showed here that a very basic clustering algorithm, k-means, leads to highly reproducible parcellation maps when applied on short fMRI time series (a few minutes) with a dynamic approach.

Another important consideration was the comparison of the reproducibility scores within and between subjects. Previous studies reported that within-subject similarity of dynamic states of parcellations was substantially higher than inter-subject similarity [17]. Our quantitative and qualitative evaluation were consistent with these findings (See Fig. 3, 4, 5 and 7) and we suggest that dynamic states of parcellations captured some of the variability between subjects. To further evaluate the reliability of these dynamic state stability maps in identifying a particular subject from a pool of subjects, we implemented a fingerprinting experiment. Even though the fingerprinting failed in a few samples, results on the ten subjects of the MSC dataset showed high accuracy results with 0.89, 0.75 and 0.73 average accuracy scores for the PCC, the dACC and the MP-VIS seeds, respectively (See Fig. 8). Researchers already demonstrated the variability in functional connectivity profiles act as a reliable fingerprinting to identify subjects from a large group [51]. Our state stability maps were derived from binary cluster maps, that eliminated a huge amount of the fine details present in a connectivity map. Despite such dramatic dimension reduction in dynamic state maps, it preserved enough relevant information to reliably delineate subjects, especially in the case of highly cognitive networks (i.e., the PCC network). Our PCC and MP-VIS accuracy scores actually outperformed the accuracy scores of connectivity maps-based fingerprinting in some networks (DMN and the salience), as reported in [52], but this observation may also reflect the fact that we used much longer individual fMRI time series and less subjects.

Another important aspect of the evaluation of the dynamic states of parcellations was their neurobiological validity. In the absence of brain organization ground truth, current parcellation work capitalized on replication, robustness and convergence as criterias for biological validity. However, the observed variations in the shape and position in the spatial patterns across individuals suggest that these patterns are likely to be associated with physiological or cognitive processes [20]. As pointed out in the previous section, our quantitative results support the neurobiological validity of our dynamic states of parcellations. Qualitatively, we observed that many regions from the dynamic states of parcellations relate to previous literature when studying network dynamics. For instance, the regions of the dACC state stability maps overlapped with the salience network regions as reported by [46] including the insula and the anterior cingulate cortex (i.e., sACC). Consistently with previous research, we frequently observed the AI and the dACC either in the primary or the secondary states of parcellations. These regions were among the most frequently activated regions in functional neuroimaging research [53,54]. In some dynamic states of parcellations, we observed a high stability around the motor and premotor regions of the dACC maps (See Fig. 4). This may be explained by the existence of a functional coupling between the AI and the dACC that facilitates a rapid access to the motor system [46]. Similarly to the dACC seed, we also observed that the PCC is multistate. In the literature, researchers observed a high spatial heterogeneity in the PCC [55,56], but in our case dynamic states were observed from a single seed and subject. Dynamic states of

parcellation of the PCC seed identified mainly ventromedial prefrontal cortex regions (i.e., including the MPFC), the superior parietal cortex regions and the precuneus. Leech and Sharp surveyed the different studies that investigated the variations in PCC activity with arousal state and its interactions with other brain networks. Authors suggested that the high heterogeneity of the PCC activity was attributed to its important role in regulating the balance between internal and external attentional focus [55]. By contrast with the dACC and the PCC seed, the MP-VIS seed was mono-state for most subjects. Consistently to resting state functional connectivity studies, the visual cortex was considered as a unimodal system since it had a maximal distance along the principal gradient between the visual and the DMN which was considered as a highly heteromodal network [56]. Overall, these qualitative observations support our hypothesis that dynamic states are driven by biological validity rather than methodological effects [20].

In addition to biological meaningful brain parcels, researchers hypothesized the existence of some non-meaningful parcels that may occur due to physiological sources or other non-neural effects such as head motion [36,55]. For the scope of this paper, we did not characterize these sources and we consider this an important follow up question to be studied for more seed regions. However, with the proposed method, a large number of time windows were not associated with a state, if no robust parcel configuration was identified. This feature of the method may help to mitigate the influence of confounding effects on dynamic brain parcellations. However, sources of physiological noise with highly consistent spatial distribution, such as cardiac noise and motion artifacts, may still lead to robust spatial parcellation states.

The most similar approach to our decomposition of brain parcels based on their dynamics is the independent component analysis (ICA) [57]. This technique identified brain networks as a temporal mixture of spatially independent components, including noise (See survey of [58]) and it was extensively applied for more than two decades in fMRI research. Based on a visual comparison of our dynamic states of parcellations and ICA spatial maps, we identified overlapping patterns especially in the case of the visual network and the default mode network including the PCC/precuneus, the MPFC regions and regions of the dorsal attentional network [59–61]. The uniform high reproducibility of our dynamic state maps for all seed regions outperformed the ICA maps reproducibility which ranged from low to medium to high measures. A major limitation of the ICA technique was the variability of functional resting state signal at the individual level added to its random initialization ([59–61]). Up to date, there are only few guidelines towards the application of ICA maps or brain atlases as a better choice to reduce the dimensionality of brain networks in neuroimaging studies [62] and, the investigation of dynamic parcels in this context represents an important direction of future research. An intriguing possibility is that dynamic parcels would converge towards similar spatial patterns as those identified by ICA, which will need to be further investigated. Both methods have indeed the ability to capture dynamic reconfiguration of brain networks, even if the underlying formalism is quite different.

Conclusion

To summarize, we show that a simple clustering technique such as k-means can lead to highly reproducible functional parcellation associated with a particular brain seed, even when applied on short fMRI time series (a few minutes). We proposed a method to identify the main states of these dynamic parcellations, and showed that their spatial distributions were subject specific. The main limitation of previous work on functional brain parcellation may be due to the over simplified static parcellation approaches. This limitation may be biasing all neuroimaging analyses that rely on static parcellation as a dimensionality reduction step, including many graph-based neuroimaging analyses. Therefore, we urge the neuroimaging scientific community to replace static brain parcellations by dynamic parcellation approaches, in order to properly capture the rich interactions between brain networks. Dynamic parcellations may thus impact widely applications of brain connectivity in health and disease.

Acknowledgements

The authors are grateful to Dr Catie Chang for providing precious feedback during early iterations of this project and to the Midnight Scan Club [15] for making MSC dataset available for our analysis. This work was funded by “The Courtois project on neuronal modelling”, based on a donation of the Courtois foundation, and funds of the Natural Sciences and Engineering Research Council (NSERC) to PB. YZ is a research fellow of the “Institut pour la valorisation des données” (IVADO). PB is a research fellow (Chercheur Boursier Junior 2) of the “Fonds de Recherche du Québec - Santé” (FRQ-S).

References

1. Braga RM, Buckner RL. Parallel Interdigitated Distributed Networks within the Individual Estimated by Intrinsic Functional Connectivity. Neuron. 2017;95: 457–471.e5.

2. Sripada C, Angstadt M, Rutherford S, Kessler D, Kim Y, Yee M, et al. Basic Units of Inter-Individual Variation in Resting State Connectomes. Sci Rep. 2019;9: 1900.

3. Nastase SA, Gazzola V, Hasson U, Keysers C. Measuring shared responses across subjects using intersubject correlation. doi:10.1101/600114

4. Betzel RF, Bertolero MA, Gordon EM, Gratton C, Dosenbach NUF, Bassett DS. The community structure of functional brain networks exhibits scale-specific patterns of variability across individuals and time. doi:10.1101/413278

5. Yaesoubi M, Adalı T, Calhoun VD. A window-less approach for capturing time-varying connectivity in fMRI data reveals the presence of states with variable rates of change. Hum Brain Mapp. 2018;39: 1626–1636.

6. Salehi M, Greene AS, Karbasi A, Shen X, Scheinost D, Todd Constable R. There is no single functional atlas even for a single individual: Parcellation of the human brain is

state dependent. bioRxiv. 2018. p. 431833. doi:10.1101/431833

7. Brodmann K. Vergleichende Lokalisationslehre der Grosshirnrinde in ihren Prinzipien dargestellt auf Grund des Zellenbaues. Barth; 1909.

8. Yeo BTT, Krienen FM, Sepulcre J, Sabuncu MR, Lashkari D, Hollinshead M, et al. The organization of the human cerebral cortex estimated by intrinsic functional connectivity. J Neurophysiol. 2011;106: 1125–1165.

9. Urchs S, Armoza J, Benhajali Y, St-Aubin J, Bellec P. MIST: A multi-resolution parcellation of functional brain networks. 2017;1: 3.

10. Glasser MF, Coalson TS, Robinson EC, Hacker CD, Harwell J, Yacoub E, et al. A multi-modal parcellation of human cerebral cortex. Nature. 2016;536: 171–178.

11. Schaefer A, Kong R, Gordon EM, Laumann TO, Zuo X-N, Holmes AJ, et al. Local-Global Parcellation of the Human Cerebral Cortex from Intrinsic Functional Connectivity MRI. Cereb Cortex. 2018;28: 3095–3114.

12. Arslan S, Ktena SI, Makropoulos A, Robinson EC, Rueckert D, Parisot S. Human brain mapping: A systematic comparison of parcellation methods for the human cerebral cortex. Neuroimage. 2017. doi:10.1016/j.neuroimage.2017.04.014

13. Thirion B, Varoquaux G, Dohmatob E, Poline J-B. Which fMRI clustering gives good brain parcellations? Front Neurosci. 2014;8: 167.

14. Nikolaidis A, Heinsfeld AS, Xu T, Bellec P, Vogelstein J, Milham M. Bagging Improves Reproducibility of Functional Parcellation. bioRxiv. 2019. p. 343392. doi:10.1101/343392

15. Gordon EM, Laumann TO, Gilmore AW, Newbold DJ, Greene DJ, Berg JJ, et al. Precision Functional Mapping of Individual Human Brains. Neuron. 2017;95: 791–807.e7.

16. Bijsterbosch JD, Woolrich MW, Glasser MF, Robinson EC, Beckmann CF, Van Essen DC, et al. The relationship between spatial configuration and functional connectivity of brain regions. Elife. 2018;7. doi:10.7554/eLife.32992

17. Kong R, Li J, Orban C, Sabuncu MR, Liu H, Schaefer A, et al. Spatial Topography of Individual-Specific Cortical Networks Predicts Human Cognition, Personality and Emotion. doi:10.1101/213041

18. Kashyap R, Kong R, Bhattacharjee S, Li J, Zhou J, Yeo T. Individual-Specific fMRI-Subspaces Improve Functional Connectivity Prediction of Behavior. doi:10.1101/515742

19. Dickie AC, Bell AM, Iwagaki N, Polgár E, Gutierrez-Mecinas M, Kelly R, et al. Morphological and functional properties distinguish the substance P and gastrin-releasing peptide subsets of excitatory interneuron in the spinal cord dorsal horn. Pain. 2019;160: 442–462.

20. Eickhoff SB, Yeo BTT, Genon S. Imaging-based parcellations of the human brain. Nat Rev Neurosci. 2018;19: 672–686.

21. Gordon EM, Laumann TO, Adeyemo B, Petersen SE. Individual Variability of the

System-Level Organization of the Human Brain. Cereb Cortex. 2017;27: 386–399.

22. Marek S, Dosenbach NUF. The frontoparietal network: function, electrophysiology, and importance of individual precision mapping. Dialogues Clin Neurosci. 2018;20: 133–140.

23. Yeo BTT, Krienen FM, Chee MWL, Buckner RL. Estimates of segregation and overlap of functional connectivity networks in the human cerebral cortex. Neuroimage. 2014;88: 212–227.

24. Hutchison RM, Womelsdorf T, Allen EA, Bandettini PA, Calhoun VD, Corbetta M, et al. Dynamic functional connectivity: promise, issues, and interpretations. Neuroimage. 2013;80: 360–378.

25. Calhoun VD, Miller R, Pearlson G, Adalı T. The chronnectome: time-varying connectivity networks as the next frontier in fMRI data discovery. Neuron. 2014;84: 262–274.

26. Allen EA, Damaraju E, Plis SM, Erhardt EB, Eichele T, Calhoun VD. Tracking whole-brain connectivity dynamics in the resting state. Cereb Cortex. 2014;24: 663–676.

27. Donnelly-Kehoe P, Saenger VM, Lisofsky N, Kühn S, Kringelbach ML, Schwarzbach J, et al. Reliable local dynamics in the brain across sessions are revealed by whole-brain modeling of resting state activity. Hum Brain Mapp. 2019;26: 63.

28. Bassett DS, Wymbs NF, Porter MA, Mucha PJ, Carlson JM, Grafton ST. Dynamic reconfiguration of human brain networks during learning. Proc Natl Acad Sci U S A. 2011;108: 7641–7646.

29. Gonzalez-Castillo J, Hoy CW, Handwerker DA, Robinson ME, Buchanan LC, Saad ZS, et al. Tracking ongoing cognition in individuals using brief, whole-brain functional connectivity patterns. Proc Natl Acad Sci U S A. 2015;112: 8762–8767.

30. Braun U, Schäfer A, Bassett DS, Rausch F, Schweiger JI, Bilek E, et al. Dynamic brain network reconfiguration as a potential schizophrenia genetic risk mechanism modulated by NMDA receptor function. Proc Natl Acad Sci U S A. 2016;113: 12568–12573.

31. Reinen JM, Chén OY, Hutchison RM, Yeo BTT, Anderson KM, Sabuncu MR, et al. The human cortex possesses a reconfigurable dynamic network architecture that is disrupted in psychosis. Nat Commun. 2018;9: 1157.

32. Liu J, Liao X, Xia M, He Y. Chronnectome fingerprinting: Identifying individuals and predicting higher cognitive functions using dynamic brain connectivity patterns. Hum Brain Mapp. 2018;39: 902–915.

33. Chen JE, Chang C, Greicius MD, Glover GH. Introducing co-activation pattern metrics to quantify spontaneous brain network dynamics. Neuroimage. 2015;111: 476–488.

34. Liu X, Duyn JH. Time-varying functional network information extracted from brief instances of spontaneous brain activity. Proc Natl Acad Sci U S A. 2013;110: 4392–4397.

35. Smith SM, Miller KL, Moeller S, Xu J, Auerbach EJ, Woolrich MW, et al. Temporally-independent functional modes of spontaneous brain activity. Proc Natl Acad Sci U S A. 2012;109: 3131–3136.

36. Chen JE, Rubinov M, Chang C. Methods and Considerations for Dynamic Analysis of

Functional MR Imaging Data. Neuroimaging Clin N Am. 2017;27: 547–560.

37. Sakoğlu U, Pearlson GD, Kiehl KA, Wang YM, Michael AM, Calhoun VD. A method for evaluating dynamic functional network connectivity and task-modulation: application to schizophrenia. MAGMA. 2010;23: 351–366.

38. Iraji A, DeRamus TP, Lewis N, Yaesoubi M, Stephen JM, Erhardt E, et al. The spatial chronnectome reveals a dynamic interplay between functional segregation and integration. bioRxiv. 2018. p. 427450. doi:10.1101/427450

39. Casorso J, Kong X, Chi W, Van De Ville D, Yeo BTT, Liégeois R. Dynamic mode decomposition of resting-state and task fMRI. Neuroimage. 2019;194: 42–54.

40. Salehi M, Karbasi A, Barron DS, Scheinost D, Todd Constable R. State-specific individualized functional networks form a predictive signature of brain state. bioRxiv. 2018. p. 372110. doi:10.1101/372110

41. Power JD, Barnes KA, Snyder AZ, Schlaggar BL, Petersen SE. Spurious but systematic correlations in functional connectivity MRI networks arise from subject motion. Neuroimage. 2012;59: 2142–2154.

42. Pedregosa F, Varoquaux G, Gramfort A, Michel V, Thirion B, Grisel O, et al. Scikit-learn: Machine Learning in Python. J Mach Learn Res. 2011;12: 2825–2830.

43. MacQueen J. Some methods for classification and analysis of multivariate observations. Proceedings of the Fifth Berkeley Symposium on Mathematical Statistics and Probability, Volume 1: Statistics. The Regents of the University of California; 1967. Available: https://projecteuclid.org/euclid.bsmsp/1200512992

44. David Arthur Stanford University, Stanford, CA, Sergei Vassilvitskii Stanford University, Stanford, CA. How slow is the k-means method? | Proceedings of the twenty-second annual symposium on Computational geometry. [cited 17 Feb 2020]. Available: https://dl.acm.org/doi/10.1145/1137856.1137880

45. Gordon EM, Laumann TO, Adeyemo B, Huckins JF, Kelley WM, Petersen SE. Generation and Evaluation of a Cortical Area Parcellation from Resting-State Correlations. Cereb Cortex. 2016;26: 288–303.

46. Menon V. Salience Network. In: Toga AW, editor. Brain Mapping. Waltham: Academic Press; 2015. pp. 597–611.

47. Menon V, Uddin LQ. Saliency, switching, attention and control: a network model of insula function. Brain Struct Funct. 2010;214: 655–667.

48. Chiong W, Wilson SM, D'Esposito M, Kayser AS, Grossman SN, Poorzand P, et al. The salience network causally influences default mode network activity during moral reasoning. Brain. 2013;136: 1929–1941.

49. Jilka SR, Scott G, Ham T, Pickering A, Bonnelle V, Braga RM, et al. Damage to the Salience Network and interactions with the Default Mode Network. J Neurosci. 2014;34: 10798–10807.

50. Kuhn HW. The Hungarian method for the assignment problem. Nav Res Logist. 2005;52: 7–21.

51. Finn ES, Shen X, Scheinost D, Rosenberg MD, Huang J, Chun MM, et al. Functional connectome fingerprinting: identifying individuals using patterns of brain connectivity. Nat Neurosci. 2015;18: 1664–1671.

52. Badhwar AP, Collin-Verreault Y, Orban P, Urchs S, Chouinard I, Vogel J, et al. Multivariate consistency of resting-state fMRI connectivity maps acquired on a single individual over 2.5 years, 13 sites and 3 vendors. doi:10.1101/497743

53. Buchsbaum BR, Greer S, Chang W-L, Berman KF. Meta-analysis of neuroimaging studies of the Wisconsin Card-Sorting task and component processes. Hum Brain Mapp. 2005;25: 35–45.

54. Yarkoni T, Poldrack RA, Nichols TE, Van Essen DC, Wager TD. Large-scale automated synthesis of human functional neuroimaging data. Nat Methods. 2011;8: 665–670.

55. Leech R, Sharp DJ. The role of the posterior cingulate cortex in cognition and disease. Brain. 2014;137: 12–32.

56. Margulies DS, Ghosh SS, Goulas A, Falkiewicz M, Huntenburg JM, Langs G, et al. Situating the default-mode network along a principal gradient of macroscale cortical organization. Proc Natl Acad Sci U S A. 2016;113: 12574–12579.

57. Calhoun VD, Adali T, Pearlson GD, Pekar JJ. Spatial and temporal independent component analysis of functional MRI data containing a pair of task-related waveforms. Hum Brain Mapp. 2001;13: 43–53.

58. Beckmann CF. Modelling with independent components. Neuroimage. 2012;62: 891–901.

59. Beckmann CF, DeLuca M, Devlin JT, Smith SM. Investigations into resting-state connectivity using independent component analysis. Philos Trans R Soc Lond B Biol Sci. 2005;360: 1001–1013.

60. Damoiseaux JS, Rombouts SARB, Barkhof F, Scheltens P, Stam CJ, Smith SM, et al. Consistent resting-state networks across healthy subjects. Proc Natl Acad Sci U S A. 2006;103: 13848–13853.

61. Zuo X-N, Kelly C, Adelstein JS, Klein DF, Castellanos FX, Milham MP. Reliable intrinsic connectivity networks: test-retest evaluation using ICA and dual regression approach. Neuroimage. 2010;49: 2163–2177.

62. Dadi K, Rahim M, Abraham A, Chyzhyk D, Milham M, Thirion B, et al. Benchmarking functional connectome-based predictive models for resting-state fMRI. Neuroimage. 2019;192: 115–134.